Mapping the effects of ozone pollution and mixing on floral odour plumes and their impact on plant-pollinator interactions

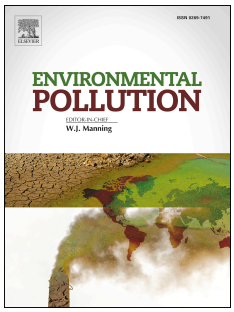

Mapping the effects of ozone pollution and mixing on floral odour plumes and their impact on plant-pollinator interactions

Ben Langford, James M.W. Ryalls, Neil J. Mullinger, Paul Hayden, Eiko Nemitz, Christian Pfrang, Alan Robins, Dalila Touhami, Lisa M. Bromfield, Robbie D. Girling

PII: S0269-7491(23)01338-6

DOI: https://doi.org/10.1016/j.envpol.2023.122336

Reference: ENPO 122336

To appear in: *Environmental Pollution*

Received Date: 5 July 2023

Accepted Date: 6 August 2023

Please cite this article as: Langford, B., Ryalls, J.M.W., Mullinger, N.J., Hayden, P., Nemitz, E., Pfrang, C., Robins, A., Touhami, D., Bromfield, L.M., Girling, R.D., Mapping the effects of ozone pollution and mixing on floral odour plumes and their impact on plant-pollinator interactions, *Environmental Pollution* (2023), doi: https://doi.org/10.1016/j.envpol.2023.122336.

Mapping the effects of ozone pollution and mixing on floral odour plumes and their impact on plant-pollinator interactions

Ben Langford[a*], James M.W. Ryalls[b], Neil J. Mullinger[a], Paul. Hayden[c], Eiko Nemitz[a], Christian Pfrang[d,e,f], Alan Robins[c], Dalila Touhami[d], Lisa M. Bromfield and Robbie D. Girling[b,g]

[a]UK Centre for Ecology & Hydrology, Penicuik, Midlothian, EH26 0QB, UK
[b]School of Agriculture, Policy and Development, University of Reading, RG6 6EU, UK
[c]EnFlo, Department of Mechanical Engineering Sciences, University of Surrey, Guildford, GU2 7XH, UK
[d]Department of Chemistry, University of Reading, P.O. Box 224, RG6 6AD, Reading, UK
[e]School of Geography, Earth and Environmental Sciences, University of Birmingham, B15 2TT, UK
[f] Department of Meteorology, University of Reading, P.O. Box 243, RG6 6BB, Reading, UK
[g]Centre for Sustainable Agricultural Systems, Institute for Life Sciences and the Environment, University of Southern Queensland, Toowoomba, Queensland 4350, Australia

*Correspondence: benngf@ceh.ac.uk

Highlights:

- Ozone pollution degrades the components of floral odour plumes
- Reaction rates were fastest at the plume edges and slowest at the plume centre
- Exposure to higher ozone concentrations increased plume intermittency and reduced odour filament width
- Honeybees recognition of floral odour plumes declined significantly following exposure of the plume to ozone

Graphical Abstract

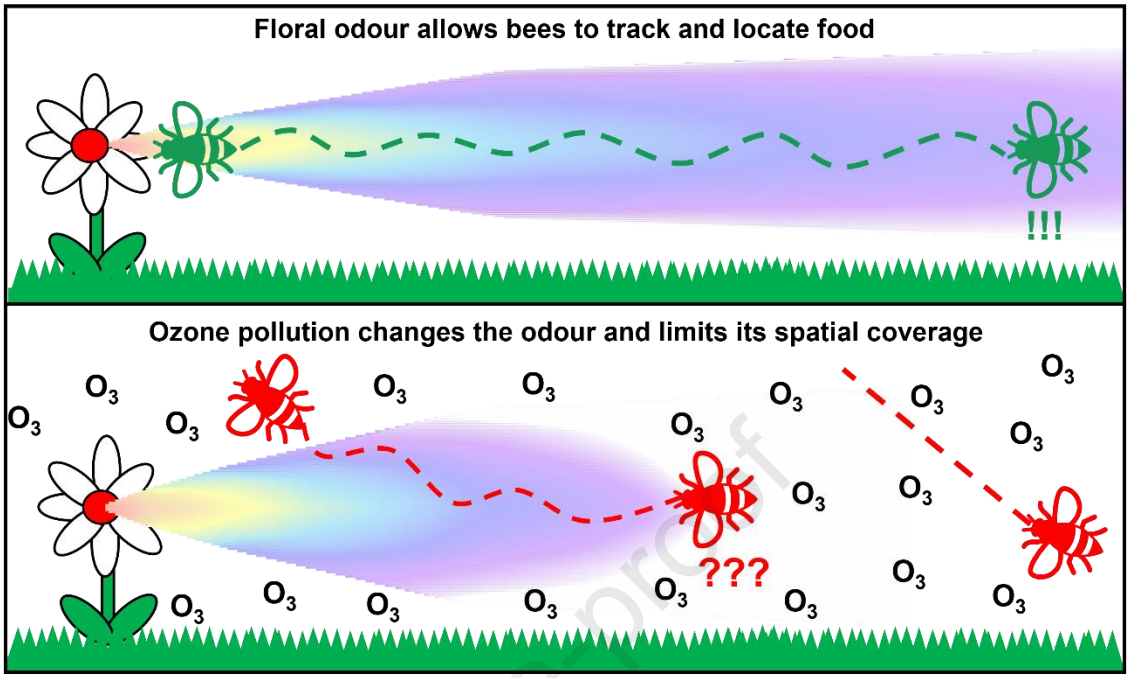

Abstract

The critical ecological process of animal-mediated pollination is commonly facilitated by odour cues. These odours consist of volatile organic compounds (VOCs), often with short chemical lifetimes, which form the strong concentration gradients necessary for pollinating insects to locate a flower. Atmospheric oxidants, including ozone pollution, may react with and chemically alter these VOCs, impairing the ability of pollinators to locate a flower, and therefore the pollen and nectar on which they feed. However, there is limited mechanistic empirical evidence to explain these processes within an odour plume at temporal and spatial scales relevant to insect navigation and olfaction. We investigated the impact of ozone pollution and turbulent mixing on the fate of four model floral VOCs within odour plumes using a series of controlled experiments in a large wind tunnel. Average rates of chemical degradation of α-terpinene, β-caryophyllene and 6-methyl-5-hepten-2-one were slightly faster than predicted by literature rate constants, but mostly within uncertainty bounds. Mixing reduced reaction rates by 8-10% in the first 2 m following release. Reaction rates also varied across the plumes, being fastest at plume edges where VOCs and ozone mixed most efficiently and slowest at plume centres. Honeybees were trained to learn a four VOC blend equivalent to the plume released at the wind tunnel source. When subsequently presented with an odour blend representative of that observed 6 m from the source at the centre of the plume, 52% of honeybees recognised the odour, decreasing to 38% at 12 m. When presented with the more degraded blend from the plume edge, recognition decreased to 32% and 10% at 6 and 12 m respectively. Our findings highlight a mechanism by which anthropogenic pollutants can disrupt the VOC cues used in plant-pollinator interactions, which likely impacts on other critical odour-mediated behaviours such as mate attraction.

Keywords: Air pollution, ozone, floral odour cues, insect pollinators, turbulent mixing.

1. Introduction

Floral odours are used by many pollinating insects to locate floral resources. Upon landing on a flower, many species of pollinating insect can learn to associate the unique blend of chemical compounds that make up the flower's odour profile with the nectar reward that it provides, facilitating them to locate rewarding flowers of the same species in the future (Jones and Agrawal, 2017). When an insect uses floral odours to locate a flower, that odour must fulfil certain criteria. For example, it must be relatively short lived, to ensure it does not accumulate, making the cue from individual flowers indistinguishable from the ambient background. At the same time, it must persist for sufficiently long to (i) reach insects and (ii) remain recognisable. Chemical communication is therefore a trade-off between short-lived cues with strong concentration gradients, and long-lived cues that travel further with weak concentration gradients (Williams and Ringsdorf, 2020).

Monoterpenes and sesquiterpenes are groups of volatile organic compounds (VOCs) which typically fulfil these criteria and are common components of floral odours (Knudsen et al., 2006).They have relatively short atmospheric lifetimes in the order of tens of minutes to several hours with respect to the hydroxyl radical (OH), the principal oxidant in the troposphere during the daytime, and with respect to NO_3 at night (Atkinson, 2000). Yet, these compounds can also be removed via reactions with ozone (O_3), a powerful oxidant formed at ground level when VOCs and oxides of nitrogen react in the presence of sunlight (Zhang et al., 2019). In the Northern hemisphere background concentrations of O_3 are in the range of 25 to 50 ppb and are further increasing at a rate of between 0.2 and 2% per year due to an increase in the emissions of its chemical precursors (Vingarzan, 2004), and local pollution episodes can see concentrations in excess of 200 ppb, particularly within or downwind of large conurbations (Group, 2021). For many monoterpenes and sesquiterpenes, reaction with O_3 is more efficient than reaction with OH, resulting in significantly shorter lifetimes. For example, α-terpinene has a lifetime of 45 minutes with respect to OH, but less than 30 s when O_3 concentrations exceed 70 ppb (Atkinson et al., 1986).

Reaction rates found in the literature assume complete mixing between VOC and oxidant, yet this may not be the case outside of the laboratory. This is particularly true for highly reactive compounds because their chemical lifetime is of the same order as the mixing time scale. This effect of spatial segregation between oxidant and VOC is often overlooked and our understanding of the applicability of reaction rates derived in a laboratory for use in the atmosphere is, therefore, uncertain.

An odour plume consists of a series of filaments, which can be considered as strands of higher concentrations of odour, that are formed by turbulent mixing. Recording VOC concentrations at any one stationary point in a plume as it moves and shifts with air movements would reveal bursts of high concentration as a filament is encountered, in-between absences of VOC, defined as the intermittency of the plume (J Murlis et al., 1992). It is this intermittency of signal that an insect's antennae encounters as it attempts to navigate upwind through to the plume's source. The combination of the constituents of an odour plume and its structure are both critical in influencing an insect's in-flight behaviour, enabling it to successfully navigate to the odour source. For example, it is well understood that male moths follow the pheromone plume of a mate by modifying their behavioural responses as a result of the frequency at which they encounter individual odour filaments (Mafra-Neto and Cardé, 1994). Similarly, the plume structure and

intermittency of plant and flower odours is important in facilitating the navigation of insects to those odour sources (Beyaert and Hilker, 2014; Riffell et al., 2014).

A recent field study using O_3 fumigation by Ryalls et al. (2022) found that the number of pollinators visiting individual flowers declined by 89% when O_3 pollution was elevated above ambient levels. One explanation for this decline was that elevated O_3 may have rapidly degraded components of the floral odour, inhibiting the ability of insects to recognize this odour and successfully locate the flower. This hypothesis was supported by the findings of a mesocosm study on the effects of ozone on the foraging behaviour of the buff-tailed bumblebee, *Bombus terrestris* (Saunier et al., 2023). A second complementary theory, is that air pollutants also cause direct oxidative stress on the insect; studies have demonstrated upregulation of proteins associated with learning and memory in the CNS of honeybees (Reitmayer et al., 2022) and olfactory coding impairment (Démares et al., 2022). It is therefore likely that both mechanisms play a part.

However, there is a gap in the mechanistic empirical evidence to explain how VOC odour degradation by O_3 occurs within an odour plume at temporal and spatial scales relevant to insect navigation and olfaction. To assess the impact of O_3 on the degradation of floral odour plumes a series of experiments were undertaken in a 20 m wind tunnel, modified to allow fumigation by O_3 to predefined levels. The study focused on four VOCs, α-terpinene, β-caryophyllene, 6-methyl-5-hepten-2-one (MHO) and linalool, which are all common components of floral odours (Knudsen et al., 2006), represent a range of atmospheric lifetimes, and have different molecular weights so are distinguishable from one another in real-time using a proton transfer reaction time-of-flight mass spectrometer. Here, we present the results for both a single compound odour plume (α-terpinene) and multicomponent odour plumes (α-terpinene, β-caryophyllene, MHO and linalool) under O_3 concentration fields of approximately 0, 50 and 150 ppb. The measured odour plumes are compared against those expected based on literature rate constants at various points within the plumes.

In addition, a separate behavioral assay was conducted to assess whether the degradation of odour plumes could affect the ability of honeybees to recognise an odour.

2. Materials and methods

2.1 Wind tunnel measurements

Measurements were made at the Natural Environment Research Council (NERC) and National Centre for Atmospheric Science (NCAS) wind tunnel facility at the University of Surrey. The Environmental Flow (EnFlo) wind tunnel is a 20 m (L) x 1.5 m (H) x 3.5 m (W), draw down design with the capability of modulating inlet flow temperature and generating specific boundary layer conditions (Carpentieri et al., 2012),(Hancock and Pascheke, 2014). Within the tunnel are two three-dimensional traversing gears, which allow the automation of sampling at specific, predefined locations. The tunnel is equipped with a gas handling system to enable the passive release of trace gases at predefined locations within the tunnel. The first seven meters of the tunnel are used to establish boundary conditions and mixing, leaving approximately 12 m of wind tunnel to perform measurements, with the final 1 m inaccessible to the 3D traverse.

A nominally 1 m deep boundary layer was generated in the wind tunnel, using a standard system of triangular spires (Irwin, 1981) and a rough surface. Previous work had established the characteristics of this boundary layer, including the variation of mean velocity, turbulence intensity and turbulence length scales with height. The experiments

used two separate release heights, 0.5 and 0.75 m. Lateral and vertical turbulence intensities at the two heights were 4.5 % and 3.2 % for the vertical component and 5.2% and 3.2 % for the lateral: length scales were similar at the two heights being 11% of the boundary layer height of ~ 1 m for the vertical component and 13% for the lateral (Carpentieri and Robins, 2015). Finally, we note that these heights are well above the near-wall, logarithmic region, which extends top about 20% of the boundary layer depth. Further rationale for the wind tunnel setup is given in Section 1.1 of the Supplementary Information (SI).

2.1.1 Ozone Fumigation

The concentration of O_3 inside the wind tunnel was controlled by releasing O_3 from a lattice manifold, which was suspended in front of the upwind air intake of the wind tunnel. The lattice comprised 35 mm diameter PVC tubing to form a 3.5 m by 1.5 m rectangle with four vertical struts at regular (0.67 m) intervals. The tubing had 5 mm diameter holes drilled at 25 mm intervals to allow for an even distribution of the O_3 into the tunnel. The O_3 concentration inside the wind tunnel was continuously monitored (2B Technologies, Model 202 Ozone Monitor) at a fixed location (see Fig. 1a) with the measured concentration used to feedback to a Proportional–Integral–Derivative (PID) controller which in turn determined the release rate of O_3 from two generators (CD1500P, ClearWater Tech, USA). Working section O_3 levels only reached target concentrations when the entire laboratory that houses the wind tunnel reached steady-state conditions. Two O_3 levels were used: ~50 ppb during the working-day, based on the ambient air quality standard (60 ppb), and 150 ppb at other times, based on the work-place standard (200 ppb). For this reason, the main fumigation experiments were conducted outside of working hours to avoid exposing laboratory users to concentrations exceeding the air quality standard. High frequency (10 Hz) measurements were also made using an O_3 monitor (Ecophysics, CLD 88 O_3) and both analysers were calibrated against an O_3 calibration source (2B Technologies, Model 306).

2.1.2 Simulated floral odour plumes

Floral odours were simulated by releasing a blend of five trace gases which ensured consistency throughout and between experiments. These included propane, an inert tracer compound with respect to O_3 (Atkinson, 2000) and four VOCs, α-terpinene, β-caryophyllene, MHO and linalool. Propane was released directly from a gas cylinder, whereas the remaining four compounds were generated using a custom-built diffusion device. Liquid standards of the four compounds were sealed in stainless steel (316 grade) diffusion tubes and placed into one of two stirred water baths (Grant Instruments, TX150, Cambridge). Oxygen free nitrogen was passed through a zero air generator (ZA FID AIR 6.0, Uvison Technologies, UK) and then flowed over the diffusion tubes at a rate of 0.3 L min^{-1}. The VOC rich air was subsequently combined with propane (UN1978 Propane, Tech Grade N1.5) and released through a ¼" diameter (O.D.) isokinetic release nozzle at a flow rate of 1 L min^{-1}. This release rate ensured the simulated floral odour exited the manifold at the same velocity as the air in the wind tunnel (~0.7 m s^{-1}) ensuring a passive release of the VOCs. The concentration of each VOC closest to the release point (x, y

coordinates of 0.5, 0 m, see Fig. 1b) was ~100 ppb for α-terpinene, 6 ppb for β-caryophyllene, 2.5 ppb for Linalool and 4.5 ppb for MHO.

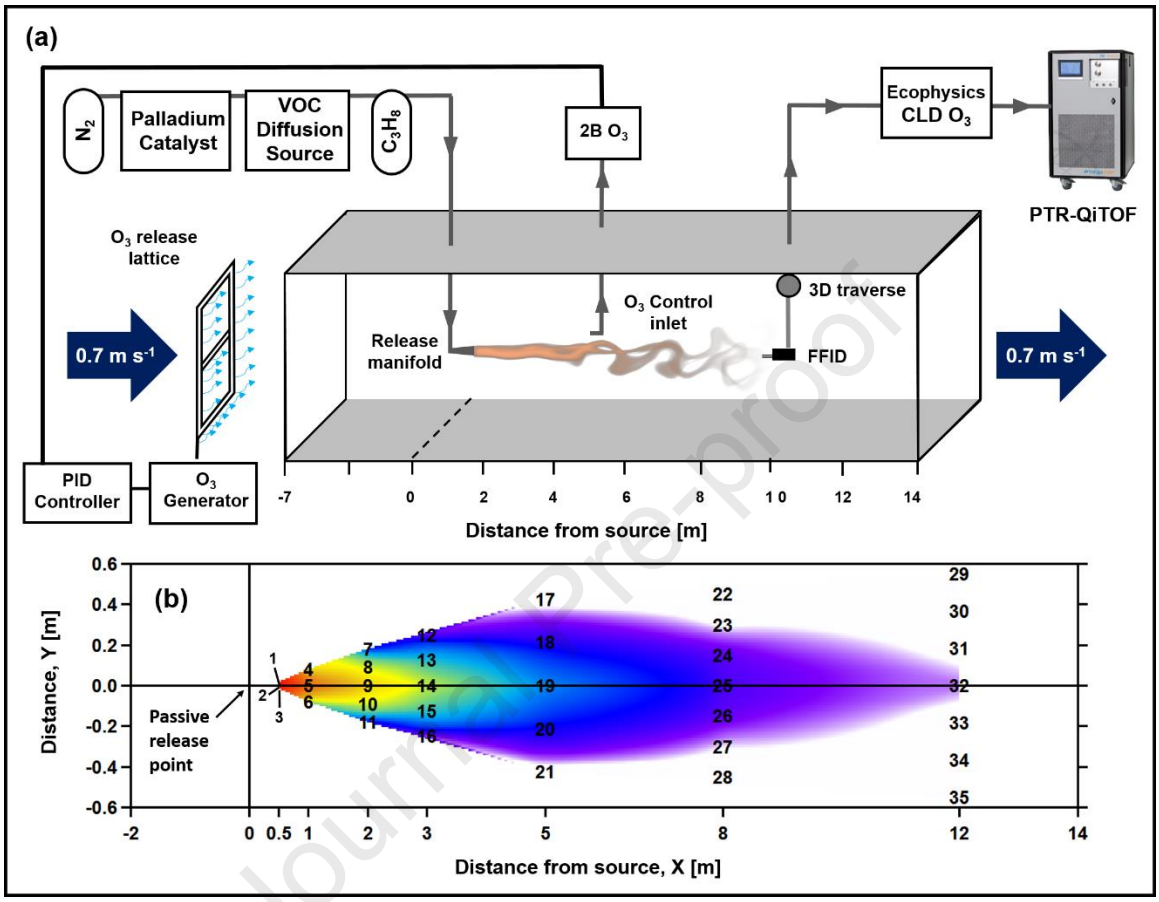

Figure 1. Schematic of the wind tunnel measurement setup (panel a) and cross-section of the wind tunnel identifying the positions of the 35 measurement locations used (panel b).

2.2 Measurement of floral odour

2.2.1 Proton transfer reaction – time-of-flight – mass spectrometer

The concentration of the VOCs within the simulated floral odour were measured using a proton transfer reaction time-of-flight mass spectrometer, with quadrupole ion guide (PTR-QiTOF, Ionicon Analytik GmbH, Austria) (Jordan et al., 2009). The conditions within the instrument's drift tube were kept constant throughout each experiment with pressure, temperature and voltage maintained at 3.8 mbar, 80 °C and 860 V, respectively. This ensured the ratio between electric field and number density of molecules (*E*/*N*) within the drift tube was maintained at 122 Td and that fragmentation of ions remained consistent. An assessment of ion fragmentation and instrument calibration is shown in Section S1.2 of the SI.

Air was sampled from the wind tunnel at a rate of ~ 6 L min^{-1} (at 500 mbar) from a ~25 m long ¼" O.D (1/8" I.D) PFA sampling line. To avoid sampling at reduced pressures, air for analysis by PTR-QiTOF was subsampled using a Teflon headed pump (KNF) to pass the air past the instrument inlet. The sample line was mounted directly to the three-dimensional traverse inside the wind tunnel and the tube heated to 80 ^{o}C to limit absorption of VOCs to the tube walls. A PTFE filter (0.45 µm pore size) was placed in line after the pump to prevent particulate matter entering the instrument. The temperature of the air within the sample line was monitored continuously and was to within 1 ˚C of the recorded wind tunnel temperature.

A Fast Flame Ionisation Detector (FFID, Cambustion, HFR400) was used to provide highly time resolved measurements of the plume structure. The frequency response of the FFID is 200 Hz and is small enough to be mounted on the traverse. The FFID operates in the range of 1000 to 0.05 ppmv. Air was sampled into the FFID along a 350 mm length of steel tubing (O.D. = 0.55 mm). The FFID was calibrated at the start of the experiment and frequent background measurements were made to allow for drift corrections which were on average less than 3%.

2.2.2 Sampling Protocol

Each plume was sampled at 35 separate locations comprising seven horizontal cross sections at 0.5, 1, 2, 3, 5, 8 and 12 m downwind of the release point (Fig. 1b). Direct measurements at point 0, 0 (co-ordinates are distances x, y in m relative to the release point and height) were not feasible and therefore measured concentrations at each location in the wind tunnel were always normalised to the 2nd measurement point (e.g. x = 0.5 m, y = 0 m), which became the effective release point.

PTR-QiTOF data were recorded with a time resolution of 10 Hz and sampled at each of the pre-defined locations for 13 minutes. This duration was found to offer a good compromise between obtaining robust statistics and ensuring all measurement locations could be sampled during the time period when O_3 fumigation in the laboratory was permitted. Following each wind tunnel measurement, the background concentration was monitored by sampling at the wind tunnel edge, outside of the plume for 1 minute. The final step was to measure the concentration of VOCs coming from the diffusion source for 1 minute, to ensure any minor deviations in release concentration could be corrected. In total, each plume characterisation experiment took approximately 9 hours to complete.

2.3 Plume intermittency and odour filament width

The intermittency of an odour plume is defined here as the fraction of time (0-1) the VOC concentration falls below the threshold of perception (ToP). This threshold is insect dependent, so here an arbitrary value defined as 1% of the 98th percentile of observed concentrations was used. The width of individual odour filaments was calculated by counting the number of consecutive measurements falling below the ToP at each location within the wind tunnel and averaging the results. The sampling rate of the PTR-QiTOF was 10 Hz and, therefore, each measurement was equivalent to a filament width of 0.1 s.

2.4 Proboscis extension response assay

To establish the effects of O_3 induced changes to the composition of floral odours on a pollinating insect's ability to successfully recognise that odour, proboscis extension response (PER) assays were performed using the western honeybee (*Apis mellifera*).

Liquid standards of the four VOCs used in the wind tunnel study were mixed into a blend, with volumes initially based on the vapour pressure of each compound (Table S1). Concentrations were assessed using a solid phase microextraction fibre (SPME) in combination with GC-MS and the methods used are outlined in Section 1.3 of the SI. Having established the initial ratio of the blend, two sets of three further odour blends were prepared aiming to replicate the ratios observed in the wind tunnel under the 150 ppb treatment at distances of 2, 6 and 12 m from the source. The first set represented the ratios seen in the plume centre and the second represent those seen at the plume edge. SPME collection and GC/MS analysis were repeated on two random blends to ensure that individual compounds were within 2% of the calculated fractions.

Proboscis Extension Response assays were conducted in an air-conditioned room at ca. 21 °C, lit by artificial light, with O_3 concentrations always at background levels (<10 ppb (Nazaroff and Weschler, 2022)). Returning forager honeybees were collected from the entrance of a hive maintained on the University of Reading's Whiteknights campus (51° 26' 9" N, 0° 56' 25" W). Individual worker bees were immobilised by cooling them on ice in 60 mL containers before being transferred and harnessed into a 1 ml pipette tip (Felsenberg et al., 2011). Only honeybees showing an initial PER elicited by 1.5 M sucrose solution were used. Each honeybee was trained to associatively learn the source VOC blend (α-terpinene, β-caryophyllene, MHO and linalool in a 1:1:1:1 ratio). Following the protocol of Matsumoto et al. (2012), honeybees were acclimatised to a continuous flow (650 mL min^{-1}) of charcoal-filtered humidified air for 25 s before being presented with the 4 s conditioned odour stimulus (i.e. an odour stream from a glass pipette containing filter paper impregnated with 20 µL of the source blend). This was immediately followed by a 3 s sucrose stimulation (unconditioned stimulus; 1.5 M sucrose solution) with a 1 s overlap, regulated by a CS-55 V2 stimulus controller (Syntech, The Netherlands). Honeybees were left in the air stream for a further 25 s after sucrose delivery to ensure that no contextual cues around the setup would be associated with the unconditioned stimulus. Honeybees were scored as having learnt the source blend if a proboscis extension was observed between odour onset and sucrose delivery. The learning trial was repeated four times for each honeybee and the inter-trial interval for each honeybee was 10 min. In the recognition trials the responses of 77 honeybees were tested to each of the six odour blends that had been prepared to replicate the VOC ratios recorded in the wind-tunnel experiments at either 2, 6 or 12 m from the source at either the plume centre or the plume edge. Recognition trials mirrored the conditioning trials, with the omission of sucrose. Extension of the proboscis within 4 s in response to the onset of the odour stimulus was classified as a positive recognition. The procedure was followed by the presentation of the source blend (0 m). Honeybees that did not extend their proboscis in response to the final conditioned stimulus (N = 6 of 77) were excluded from analysis. As such, 34 and 37 individuals responding to VOC blends at the plume centre and plume edge, respectively (71 honeybees in total), were incorporated in statistical analyses (see Section 1.4 of the SI).

3. Results and discussion

3.1 Wind tunnel plume measurements

3.1.1 α-terpinene plume

A single component release of α-terpinene was used to map out the spatial distribution of an odour plume and to determine how this changed under differing levels of O_3 pollution. Figure 2 shows the measured odour plumes under O_3 fields of 0 (Fig. 2a), 50 (Fig. 2b), and 150 ppb (Fig. 2c). Background O_3 levels within the wind tunnel were between 8 and 12 ppb and therefore a true 0 ppb field could not be achieved. Instead, Fig. 2a shows a plume of propane, which does not react with O_3 and can therefore be considered representative of the α-terpinene plume injected into a zero O_3 concentration field.

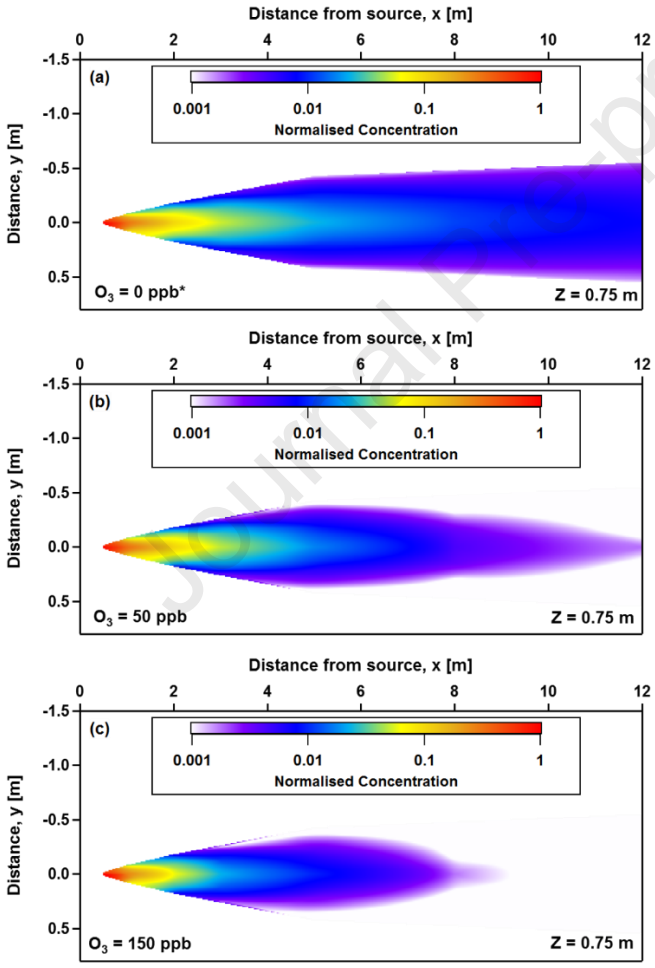

Figure 2. Horizontal plume cross sections showing the concentration of α-terpinene normalised to the point closest to the odour plume source for ozone (O_3) fields of ~0 (panel a), ~50 (panel b) and ~150 ppb (panel c). The colour scale of each plume has been log normalised. * Panel a shows a plume of propane, which does not react with O_3 and can, therefore, be considered representative of the α-terpinene plume injected into a zero O_3 concentration field.

Each plot consists of the 35 individual measurement points (shown in Figure 1b) which have subsequently been interpolated using the "natural neighbour" approach and Voroni tessellation (See "image_interpolate" function, Igor Pro, Version 8.0.3.3, Wavemetrics). Similar plots showing the average O_3 concentration are shown in the Supplementary Information (figure S1).

For each experiment the wind tunnel was operated using a standard 1 m boundary layer. which resulted in a wind speed of 0.68 m s^{-1} at the 0.75 m height and 0.63 m s^{-1} at the 0.5 m measurement height, equivalent to travel times of ~16.9 and 18.25, respectively, between the effective release point and the end of the wind tunnel. Figure 2a, where no ozonolysis occurs, demonstrates the effect of dilution on the plume, concentrations dropping to < 1% of the effective release point by the time the air exits the wind tunnel.

The addition of O_3 to the wind tunnel changed the plume shape causing a narrowing as the α-terpinene mixed with the O_3 rich air at the plume edges. Figure 2b shows that ozonlysis removed almost all of the α-terpinene in the 16 s that it took for plume to travel the length of the wind tunnel at 50 ppb of O_3, and at 150 ppb (Fig. 2c), all of the α-terpinene had reacted away by 9.5 m (13.5 s). These two-dimensional cross sections demonstrate how a plumes spatial extent, both length and width, can be significantly reduced under increasing levels of O_3 pollution at concentrations regularly observed in the lower troposphere at background levels (50 ppb) and also during elevated pollution episodes (150 ppb) (Group, 2021).

The α-terpinene plumes were also modelled by subtracting the expected chemical loss from the conserved propane plume. Theoretical first-order loss rates were calculated as

$$Loss = \left(\frac{t}{t_{loss}}\right), \quad (2)$$

where t is the time since release into the O_3 field in seconds and t_{loss} is the total loss rate of VOC with respect to O_3 calculated as

$$t_{loss=}\left(\frac{\left(k_{AT,O_3}\right)^{-1}}{[O_3]}\right). \quad (3)$$

Here, $k_{AT,O3}$, is the ozonolysis rate constant (see Table S1) and [O_3] was the concentration of O_3 measured at each location in the wind tunnel in molecules cm^{-3}. The time since release was calculated based on the straight-line distance between the effective release and measurement point and the fixed wind speed.

Figure 3, panels a and b show the percentage difference between measured and theoretical plumes for the ~50 and ~150 ppb O_3 fields, respectively. In both cases, the measured plume is degraded more quickly than would be expected based on the literature rate constant: an average of 21% for 50 ppb and 24% for 150 ppb, based on the measured data points, only. This was partially explained by the additional time available for reaction as sampled air was drawn into the PTR-QiTOF. A cross-covariance function applied to the propane signal measured *in situ* by the FFID (and used for the theoretical plume calculations) and PTR-QiTOF showed this delay to be ~1.6 s (see Figure S2 of the SI).

Accounting for this additional delay reduced the average difference to 18% and 12%, for 50 ppb and 150 ppb scenarios, respectively.

The overall increased reaction rates may be influenced by additional chemical sinks in the wind tunnel including reactions with either OH or NO_3, which were not measured during the study. The spatial behaviour of the plume supports the view that imperfect mixing affects the rate constant: the difference plots highlight the increased reaction rate at the plume edges, where mixing between O_3 and the VOC is particularly efficient, but less change is seen at the plume centre. The reaction rate appears slowest during the first 0.5 to 2 m after release, which is consistent with the limited opportunity for mixing shortly after release. Incomplete mixing reflects the intensity of segregation between the O_3 and VOCs,

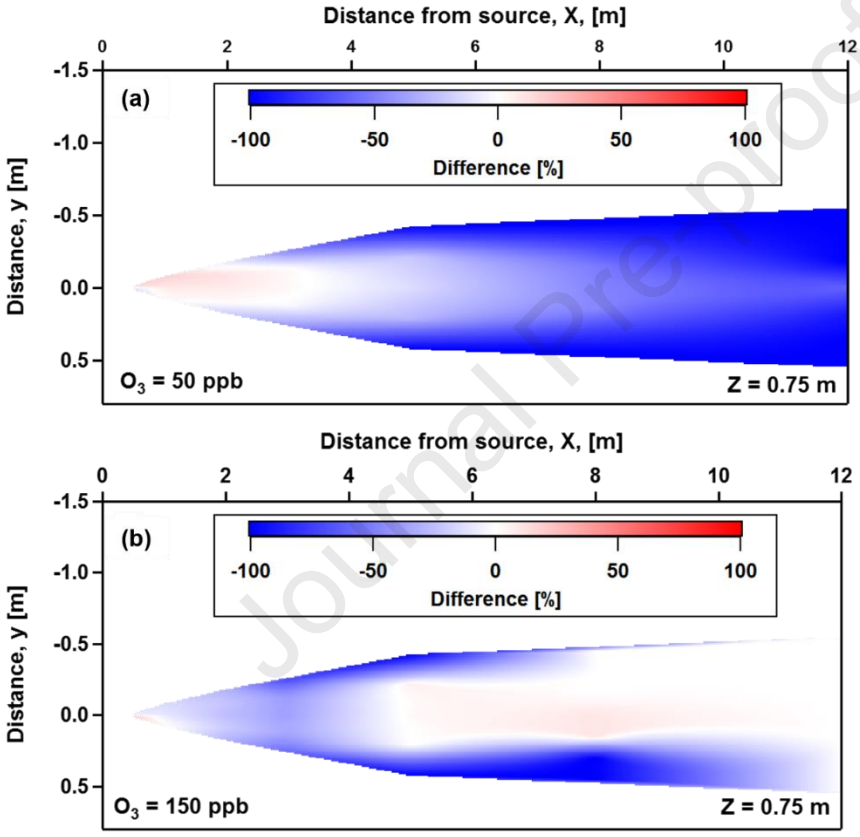

Figure 3 shows the percentage difference between an a-terpinene plume predicted based on literature rate constants and that measured by the PTR-QiTOF (e.g. measured – predicted)/predicted). Panel a and b show the difference plot under ozone conditions of 50 ppb and 150 ppb of ozone, respectively. Both plumes were released from a height of 0.75 m.

which effectively reduces the rate constant and increases the lifetime of the compound. The rate of change of VOC concentration with respect to O_3 can be calculated as

$$\frac{\partial[VOC]}{\partial t} = -k_{VOC,O3}([O_3][VOC] + [O_3'VOC']), \quad (4)$$

where square brackets represent averages and the primes denote deviations from the mean concentration. Using the measured α-terpinene and O_3 concentrations, both measured at 10 Hz, the effective rate coefficient ($k_{eff,AT,O3}$) can be calculated following the approach of Krol et al. (2000) and Pugh et al. (2010), where the intensity of segregation, *S*, between O_3 and α-terpinene is defined as

$$S_{AT,O_3} = \frac{[O_3' AT']}{[O_3][AT]}. \quad (5)$$

This intensity of segregation can be used to derive an effective rate constant as:

$$k_{eff,AT,O3} = k_{AT,o_3}(1 + S_{AT,O_3}). \quad (6)$$

Figure 4, panel (a) shows the effective rate constant for α-terpinene, calculated based on the α-terpinene plume released at a height of 0.75 m into an O_3 field of 150 ppb. The literature rate constant for α-terpinene is 2.1 x 10^{-14} cm^3 $molecule^{-1}$ s^{-1}, and the effective rate constant is roughly equivalent to this at the plume centre between 4 and 8 m. However, at the effective release point (y=0, x=0.5), $k_{eff,AT,O3}$ is decreased by ~8%, thereby increasing the lifetime of α-terpinene at that point. Towards the plume edges, from 3 m down the tunnel and beyond, $k_{eff,AT,O3}$ is closer to $k_{AT,}$ than at the plume centre where there the α-terpinene has less opportunity to mix with the O_3.

Repeating the same experiment at the lower height of 0.5 m (Figure 4b), where turbulence is slightly increased, showed a somewhat steeper gradient in the effective rate constant, with up to a 10% reduction at the effective release point. This is counter to expectation because the increased turbulence and longer travel time should enhance mixing and reduce the effects of segregation. Figure 3c shows the effective rate constant for both measurement heights at each location within the tunnel. There is a small difference between the effective rate constants measured at 0.5 and 1 m but this was within the uncertainty bounds which was based on the standard deviation of the measurements. This potentially reflects the fact that differences in the turbulence intensities between the two heights was relatively minor (4.5 % and 3.2 % for the vertical component and 5.2% and 3.2 % for the lateral). Further measurements at lower heights were not possible due to the potential for the plume to interact with the wind tunnel's surface.

A maximum 8-10% decrease of the rate constant may appear modest, but it should be viewed as a lower limit. This is because our instruments were limited to a frequency response of 10 Hz. Comparison of the PTR-QiTOF measurements with those of propane made by the FFID at a frequency of 200 Hz, revealed fine scale variation in concentration that is lost when using a 10 Hz measurement (see Fig. S3). Therefore, the effects of segregation could be greater; particularly for an insect encountering the plume, whose antennae can detect changes at a rate far greater than 10 Hz (Szyszka et al., 2014).

This result indicates that mixing plays an important, but often overlooked, role in the lifetime of VOCs. For those VOCs used as chemical cues, this is particularly important because the short lifetimes necessary to generate strong concentration gradients mean the lifetime of the signal compound is invariably similar to, or shorter than, the mixing time scale.

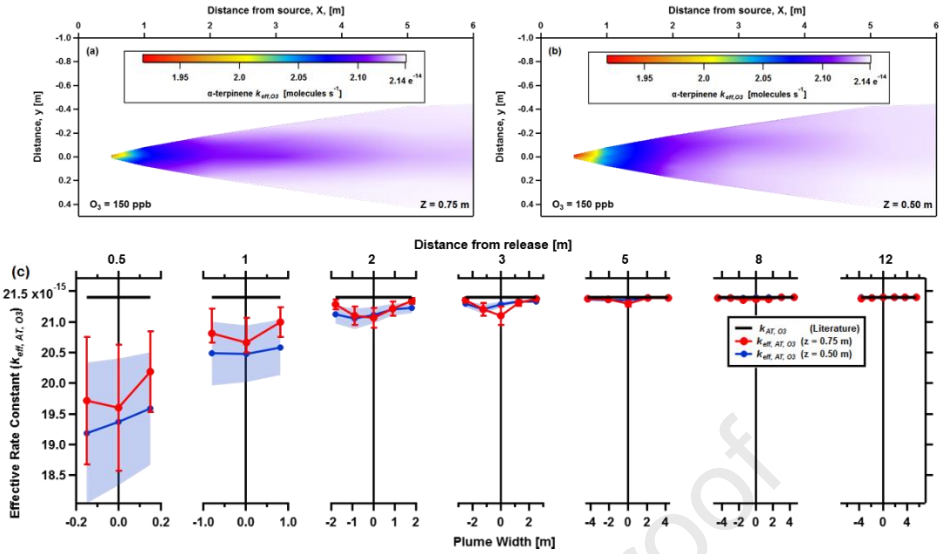

Figure 4. The effective rate constant ($k_{eff,O3}$) for α-terpinene measured at 0.75 m (panel a) and 0.5 m (panel b) above ground level when released into an ozone field of 150 ppb. Panel c shows the measured effective rate constant at each point within the wind tunnel at the two measurement heights together with the uncertainty (red line = 0.75 m, blue line = 0.5 m). The literature rate constant, k_{O3}, is 2.14 x 10^{-14} (black line). Turbulence levels were 3-5% higher both laterally and vertically for the 0.5 m height.

3.1.2 Multi-component plume

Cross sectional plots of each individual component of the multicomponent release, which is more representative of a floral odour plume, showed variations in the reaction rates of the four VOCs: α-terpinene, β-caryophyllene, MHO and linalool (see Fig. S4 a-d). The difference between the theoretical and measured plumes are shown in Figure 5 and a more detailed comparison that incorporates the uncertainty of the literature rate constants is shown in Figures S5-S8. For α-terpinene, β-caryophyllene and MHO, the measured plumes are again degraded faster than would be expected based on their respective O_3 rate constants, with the largest differences occurring at the plume edge. Applying a correction for the additional sampling delay accounted for 7% and 4% of the difference for α-terpinene, β-caryophyllene, respectively, and less than 1% for MHO. As was the case for a-terpinene, the reason for the reaction rates exceeding those expected based on literature rate constants, even despite the effects of segregation, likely relates to the presence of OH and or NO_3 within the wind tunnel.

Linalool is degraded more slowly than implied by its rate constant and the difference becomes larger towards the plume edge. It is likely that an oxidation product, from either α-terpinene or β-caryophyllene is formed which contributes to the linalool signal, most likely as a fragment ion. This is supported by the fact that the difference is largest at the plume edge where the mixing and hence reaction rates are at their fastest.

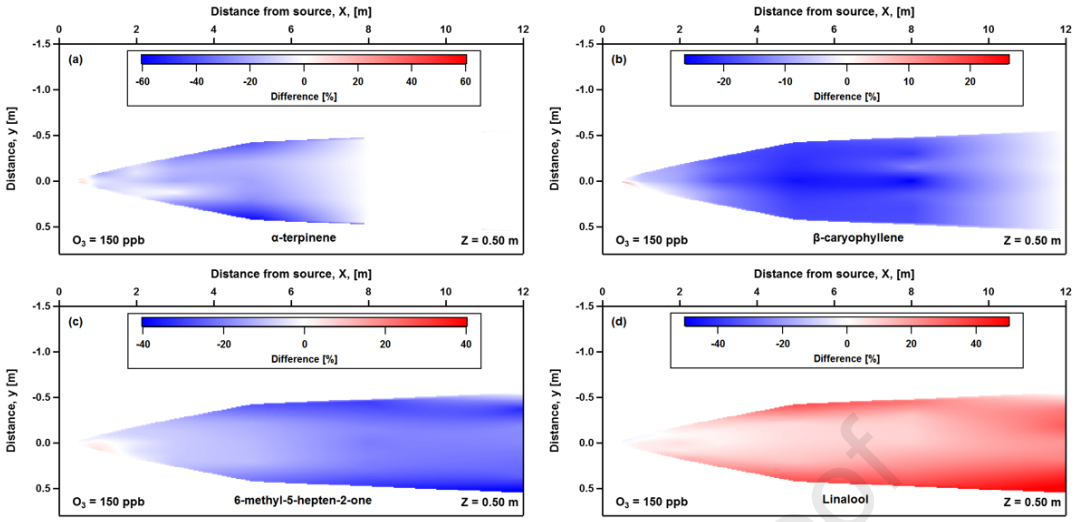

Figure 5 shows the percentage difference between VOC plumes that has been predicted based on literature reaction rates with O_3, and that measured by PTR-QiTOF (e.g. (measured – predicted)/predicted) Panel a-d show the results for a-terpinene (a), b-caryophyllene (b), MHO (c) and linalool (d). The odour plume was released from a height of 0.5 m into an ozone field of 150 ppb.

3.2 Effect of ozone on plume intermittency and odour filament width

Plume intermittency is considered to be a function of source strength and turbulent mixing. Yet. Figure 6 shows that higher levels of O_3 caused an increase in intermittency and reduction in odour filament width of an α-terpinene plume when released under identical turbulent profiles. These changes are likely to have behavioural consequences for a flying insect using the odour plume to navigate to a source. Both factors are critical in eliciting insect flight behaviours and small changes to plume structure can have dramatic effects on flight behaviour and the ability of a foraging insect to locate an odour source (Beyaert and Hilker, 2014; Mafra-Neto and Cardé, 1994) However, we did not directly investigate the effects of the changes we observed to intermittency and filament number on insect flight behaviour and therefore the degree of impact of those changes remains unclear. Again, the largest changes in intermittency and odour filament width were observed towards the outer edges of the plume where mixing with O_3 is most efficient.

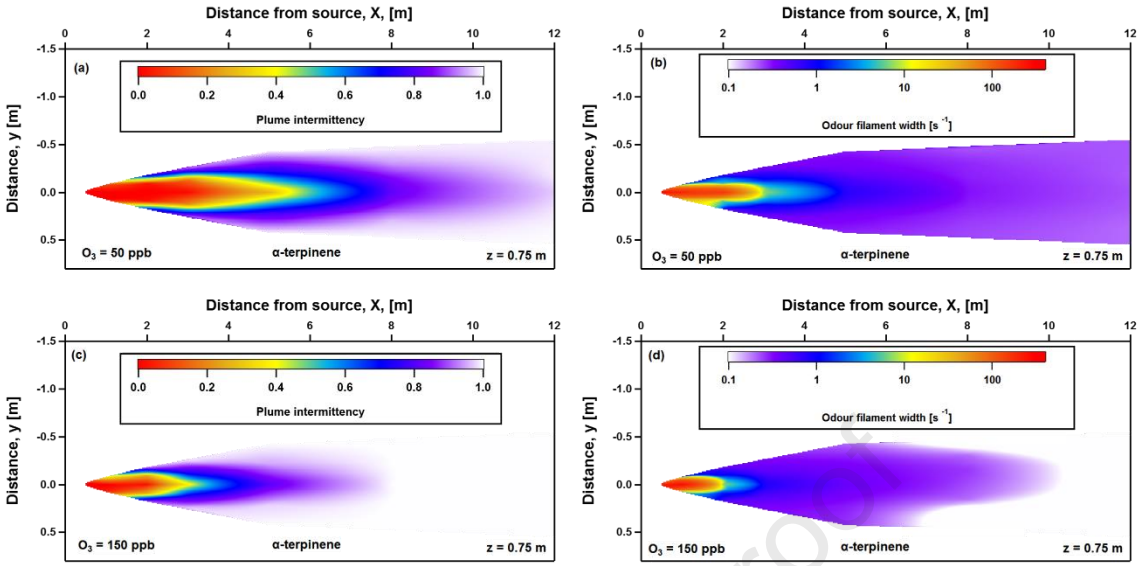

Figure 6, panels a and c, show the intermittency of an a-terpinene plume, defined as the fraction of time (0-1) that the measured signal fell below the threshold of perception (see text for definition), under identical turbulent conditions but varying ozone concentrations of 50 ppb and 150 ppb, respectively. Panels b and d show the average odour filament width from the same a-terpinene plumes. Note the colour scale in panels b and d are shown on a logarithmic scale.

3.3 Honeybee Proboscis Extension Response (PER) Assays

Figure 7 shows the ratios recoded in the wind-tunnel under 150 ppb of O_3, and those reproduced for the PER assays. Panels a versus c show the plume centre and b versus d show the plume edge. The ratios were not identical but provided a reasonable approximation of the composition change observed in the wind tunnel.

When honeybees were presented with the VOC odour profile they had been trained to (i.e. the profile representative of the VOC blend at the tunnel source, or 0 m), 100% showed a positive PER response (Figure 7 c and d), i.e. all individuals recognised the blend to which they had been trained. However, for the less degraded central plume (figure 7 c), when honeybees were presented with a VOC blend representative of that recorded at 6 m from the tunnel odour source only 52% of honeybees tested exhibited a positive PER response, decreasing to 38% for bees presented with the VOC blend representative of 12 m from the odour source. For the honeybees presented with VOC blends representing the more degraded plume edge (Figure 7 d), just 32% responded to that representing 6 m from the odour source, decreasing to 10% to the blend representing 12 m from the odour source. Overall, significantly fewer honeybees responded to the VOC blend at the plume edge compared with the plume centre (χ^2_1 = 9.56, P = 0.002) and significantly fewer honeybees responded as the distance from the source increased (χ^2_1 = 39.17, P < 0.001). There was no significant two-way (Location x Distance) interaction (χ^2_1 = 9.56, P = 0.002. These results suggests that changes in VOC ratios resulting from O_3 pollution and at fairly small foraging distances from a floral odour source could cause large reductions in the ability of honeybees to be able to recognise a floral blend, potentially disrupting the processes pollinating insects rely on for location of floral food resources. This supports previous findings of behavioural studies, which have

demonstrated changes in insect behaviour (Vanderplanck et al., 2021) (Saunier et al., 2023) and reduced pollination of flowers under elevated O_3 (Ryalls et al., 2022).

It should be noted that this assay purely assessed the honeybee's abilities to recognise the odour and therefore, the results do not capture any additional effects associated with direct exposure to O_3. Furthermore, here the honeybees are responding to a mean concentration, and therefore, the additional impact of O_3 on the spatial extent and intermittency of the plume as well as the odour filament width are not captured within the honeybees response.

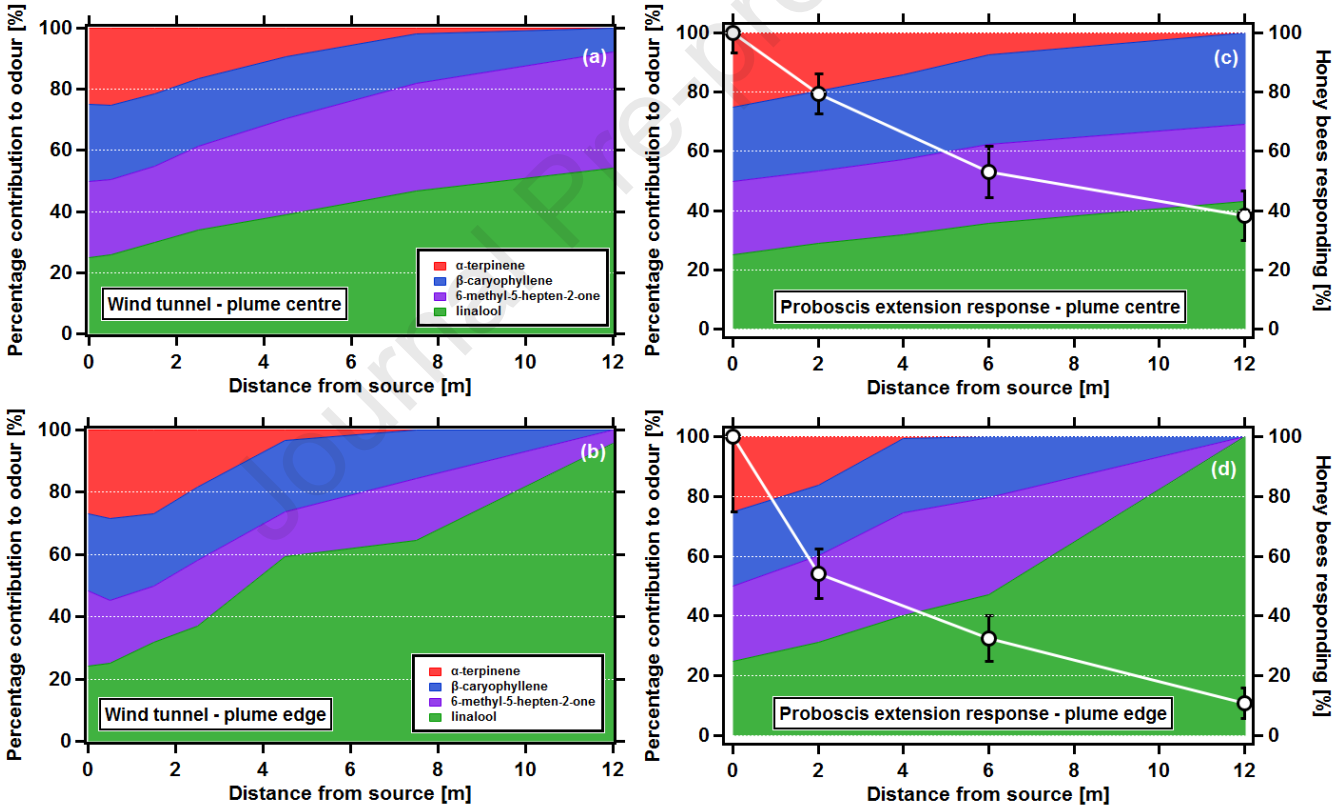

Figure 7 Observed ratios of α-terpinene, β-caryophyllene, 6-methyl-5-hepten-2-one (MHO) and linalool measured at the plume centre (panel a) and plume edge (panel b) under an ozone field of 150 ppb. Panels c and d show an attempt to replicate these ratios as part of a proboscis extension response assay, for the plume centre and plume edge, respectively. The right hand axis and line graphs on panels c and d indicate the percentage of forager honeybees which, after learning the four VOC blend representative of 0 m from the source, extended their proboscis (indicating recognition) when presented with VOC blends representative of 2, 6 and 12 m from the source (± S.E.). Data are expressed as the percent PER recognition of each distance relative to the PER recognition of blend at the source ((n = 34 and 37 individuals for the plume centre and plume edge, respectively). While there was no significant two-way interactive effect of 'distance from the source' and 'location of the plume', both were individually significant. As such, significantly fewer honeybees responded to the VOC blend corresponding to the

plume edge compared with the plume centre (z = -2.814, P < 0.005) and honeybee responses significantly decreased from 2 to 6 m (z = -3.39, P = 0.001) and from 6 to 12 m (z = -2.82, P = 0.005) according to post-hoc tests.

4. Conclusions

Controlled releases of both single and multiple component synthetic floral odours were measured in a wind tunnel under differing levels of O_3. The rate of reaction of each compound (α-terpinene, β-caryophyllene, MHO and linalool) were found to be broadly similar to that expected based on literature rate constants, but in most cases slightly faster, likely due to additional chemical sinks (e.g. OH and NO_3) for the VOCs within the wind tunnel. The notable exception was linalool, where reaction rates were slower than expected. In this case, fragmentation of an oxidation product to *m/z* 155 was thought to be the most likely cause.

An analysis of the intensity of segregation between the concentrations of α-terpinene and O_3 revealed that the effective rate constant ($k_{eff,AT,O3}$) was reduced by up to 10% in the first 2 m following release. The effect of segregation was expected to decrease at lower measurement heights, but no statistically significant difference was observed between the 0.75 and 0.5 m measurements. This reflected the small differences in turbulence intensity between these two measurement heights. Reaction rates were fastest at the plume edges attributed to the increased opportunity to mix with ozone. Ozone was also found to increase the intermittency of the plume and decrease odour filament width, two properties used by insects for navigation.

Replication of the average plume composition in a proboscis response assay clearly showed a rapid decline in honeybees' ability to recognise the floral odour following simulated degradation by O_3. These results, although based upon a synthetic odour, provide an important insight into the mechanism by which anthropogenic pollutants can disrupt the chemical cues used by insects. Importantly, our experimental approach, where the effects of O_3 degradation were replicated and then presented to the insect, allows its effects to be de-coupled from potential olfactory coding impairment caused by direct oxidative stress. In this instance, the effects are pronounced within just a short distance from the point of release.

However, outside of the laboratory, the extent to which ozonolysis impacts on pollinators will ultimately depend on the reactivity of the components within a given floral odour, the ambient O_3 concentration (and NO_3 if at night-time) and wind speed. Nonetheless, our work demonstrates a clear mechanism, capable of explaining the large decline in pollinator visits seen in previous field scale O_3 fumigation studies (Ryalls et al., 2022) which may also be relevant for other odour-mediated behaviours such as mate attraction.

Acknowledgments

We thank Paul Nathan and Zoe Ansell for technical support during the wind tunnel studies. Thanks to Helen Dominick for assistance collecting honeybees. Thanks to Dr Stephen Elmore for support during the GC-MS studies.

Funding

This work was funded by the Natural Environmental Research Council (NERC) through the project Degradation of Odour signals by air pollution: chemical Mechanisms, plume dynamics and Insect-Orientation behaviour (DOMINO, NE/P001971/2) and the PTR-QiToF instrument through grant NE/P016502/1

Declaration of competing interest

The authors declare that they have no known competing financial interests or personal relationships that could have appeared to influence the work reported in this paper.

Data availability

Data is available upon reasonable request.

Author statement

RG, BL, CP and EN obtained the funding, BL, NJM, DT, RG, CP, EN, PH and AR performed the wind tunnel study. JR, LB and RG performed the proboscis extension response assays and all authors contributed to the writing of the manuscript.

References

Atkinson, R., 2000. Atmospheric chemistry of VOCs and NOx. Atmospheric Environment 34, 2063-2101.

Atkinson, R., Aschmann, S.M., Pitts Jr., J.N., 1986. Rate constants for the gas-phase reactions of the OH radical with a series of monoterpenes at 294 ± 1 K. International Journal of Chemical Kinetics 18, 287-299.

Beyaert, I., Hilker, M., 2014. Plant odour plumes as mediators of plant-insect interactions. Biol Rev Camb Philos Soc 89, 68-81.

Carpentieri, M., Hayden, P., Robins, A.G., 2012. Wind tunnel measurements of pollutant turbulent fluxes in urban intersections. Atmospheric Environment 46, 669-674.

Carpentieri, M., Robins, A.G., 2015. Influence of urban morphology on air flow over building arrays. Journal of Wind Engineering and Industrial Aerodynamics 145, 61-74.

Démares, F., Gibert, L., Creusot, P., Lapeyre, B., Proffit, M., 2022. Acute ozone exposure impairs detection of floral odor, learning, and memory of honey bees, through olfactory generalization. Science of the Total Environment 827, 154342.

Felsenberg, J., Gehring, K.B., Antemann, V., Eisenhardt, D., 2011. Behavioural pharmacology in classical conditioning of the proboscis extension response in honeybees (Apis mellifera). J Vis Exp.

Group, A.Q.E., 2021. Ozone in the UK - recent trends and future projections, pp. 1-143.

Hancock, P.E., Pascheke, F., 2014. Wind-tunnel simulation of the wake of a large wind turbine in a stable boundary layer. Part 1: the boundary-layer simulation. Boundary-Layer Meteorology 151, 3+.

Irwin, H.P.A.H., 1981. The design of spires for wind simulation. Journal of Wind Engineering and Industrial Aerodynamics 7, 361-366.

J Murlis, J S Elkinton, a., Cardé, R.T., 1992. Odor Plumes and How Insects Use Them. Annual Review of Entomology 37, 505-532.

Jones, P.L., Agrawal, A.A., 2017. Learning in Insect Pollinators and Herbivores. Annual Review of Entomology 62, 53-71.

Jordan, A., Haidacher, S., Hanel, G., Hartungen, E., Mark, L., Seehauser, H., Schottkowsky, R., Sulzer, P., Mark, T.D., 2009. A high resolution and high sensitivity proton-transfer-reaction time-of-flight mass spectrometer (PTR-TOF-MS). International Journal of Mass Spectrometry 286, 122-128.

Knudsen, J.T., Eriksson, R., Gershenzon, J., Ståhl, B., 2006. Diversity and distribution of floral scent. The Botanical Review 72, 1.

Krol, M.C., Molemaker, M.J., de Arellano, J.V.G., 2000. Effects of turbulence and heterogeneous emissions on photochemically active species in the convective boundary layer. Journal of Geophysical Research: Atmospheres 105, 6871-6884.

Mafra-Neto, A., Cardé, R.T., 1994. Fine-scale structure of pheromone plumes modulates upwind orientation of flying moths. Nature 369, 142-144.

Matsumoto, Y., Menzel, R., Sandoz, J.-C., Giurfa, M., 2012. Revisiting olfactory classical conditioning of the proboscis extension response in honey bees: A step toward standardized procedures. Journal of Neuroscience Methods 211, 159-167.

Nazaroff, W.W., Weschler, C.J., 2022. Indoor ozone: Concentrations and influencing factors. Indoor Air 32, e12942.

Reitmayer, C.M., Girling, R.D., Jackson, C.W., Newman, T.A., 2022. Repeated short-term exposure to diesel exhaust reduces honey bee colony fitness. Environmental Pollution 300, 118934.

Riffell, J.A., Shlizerman, E., Sanders, E., Abrell, L., Medina, B., Hinterwirth, A.J., Kutz, J.N., 2014. Flower discrimination by pollinators in a dynamic chemical environment. Science 344, 1515-1518.

Ryalls, J.M.W., Langford, B., Mullinger, N.J., Bromfield, L.M., Nemitz, E., Pfrang, C., Girling, R.D., 2022. Anthropogenic air pollutants reduce insect-mediated pollination services. Environmental Pollution 297, 118847.

Saunier, A., Grof-Tisza, P., Blande, J.D., 2023. Effect of ozone exposure on the foraging behaviour of Bombus terrestris. Environmental Pollution 316, 120573.

Szyszka, P., Gerkin, R.C., Galizia, C.G., Smith, B.H., 2014. High-speed odor transduction and pulse tracking by insect olfactory receptor neurons. Proceedings of the National Academy of Sciences 111, 16925-16930.

Vanderplanck, M., Lapeyre, B., Brondani, M., Opsommer, M., Dufay, M., Hossaert-McKey, M., Proffit, M., 2021. Ozone Pollution Alters Olfaction and Behavior of Pollinators. Antioxidants 10, 636.

Vingarzan, R., 2004. A review of surface ozone background levels and trends. Atmospheric Environment 38, 3431-3442.

Williams, J., Ringsdorf, A., 2020. Human odour thresholds are tuned to atmospheric chemical lifetimes. Philosophical Transactions of the Royal Society B: Biological Sciences 375, 20190274.

Zhang, J., Wei, Y., Fang, Z., 2019. Ozone Pollution: A Major Health Hazard Worldwide. Frontiers in Immunology 10.

Highlights:

- Ozone pollution degrades the components of floral odour plumes
- Reaction rates were fastest at the plume edges and slowest at the plume centre
- Higher O_3 levels increased plume intermittency and reduced odour filament width
- Bees recognition of floral odours declined significantly following reaction with O_3

Declaration of interests

☒ The authors declare that they have no known competing financial interests or personal relationships that could have appeared to influence the work reported in this paper.

☐The authors declare the following financial interests/personal relationships which may be considered as potential competing interests: